An Econometric Model for Intraday Electricity Trading

Marcel Kremer[*,a], Rüdiger Kiesel[a,b], and Florentina Paraschiv[c,d]

[a]*Chair for Energy Trading and Finance, University of Duisburg-Essen, Universitätsstraße 12, 45141 Essen, Germany*
[b]*Department of Mathematics, University of Oslo, PO Box 1053 Blindern, 0316 Oslo, Norway*
[c]*NTNU Business School, Norwegian University of Science and Technology, 7491 Trondheim, Norway*
[d]*Institute for Operations Research and Computational Finance, University of St. Gallen, Bodanstrasse 6, CH-9000 St. Gallen, Switzerland*

May 11, 2020

Revised version forthcoming in *Philosophical Transactions of the Royal Society A*.

Abstract

This paper develops an econometric price model with fundamental impacts for intraday electricity markets of 15-minute contracts. A unique data set of intradaily updated forecasts of renewable power generation is analyzed. We use a threshold regression model to examine how 15-minute intraday trading depends on the slope of the merit order curve. Our estimation results reveal strong evidence of mean reversion in the price formation mechanism of 15-minute contracts. Additionally, prices of neighboring contracts exhibit strong explanatory power and a positive impact on prices of a given contract. We observe an asymmetric effect of renewable forecast changes on intraday prices depending on the merit-order-curve slope. In general, renewable forecasts have a higher explanatory power at noon than in the morning and evening, but price information is the main driver of 15-minute intraday trading.

Keywords: Intraday electricity market; Econometric modeling; 15-minute contracts; Renewable power forecasts; Merit order curve; Threshold regression

JEL Classification: C22; C24; C55; G10; Q20; Q21; Q40; Q41; Q42

1 Introduction

In recent years, the expansion of renewable energy sources has been forged ahead massively across the globe with a direct impact on electricity markets. As electricity generation from renewable energy sources cannot be predicted reliably in the long-term, that is, days, weeks or months ahead, the future of electricity trading is foreseen in short-term electricity markets.

[*]Corresponding author. Email: marcel.kremer@uni-due.de

Energy supply companies thus face the challenge of moving towards automatic trading, which requires the identification of trading strategies based on local demand and supply patterns as well as cross-border energy flows. The German market constitutes a pioneer among European electricity markets. Not only is the German market the largest electricity market in Europe in terms of total trading volume (European Energy Exchange AG, 2016a), but also novel developments and innovations (new contracts, reduction of lead time) are traditionally introduced on the German market first. In Germany the most short-term electricity market is the continuous intraday market, where hourly and 15-minute contracts can be traded until five minutes before the delivery of electricity begins. Intraday electricity markets are designed according to the needs of energy supply companies to balance forecast errors of renewable power generation.

This paper investigates four research questions: (i) Which fundamental factors drive the intraday trading of 15-minute contracts? (ii) How do forecast changes of renewable power generation affect the intraday trading of 15-minute contracts? (iii) Can we identify different regimes on the intraday market where the price formation process behaves differently? (iv) How does intraday trading depend on the time of day?

Like on any financial market, there is a natural desire for pricing models of the basic securities. To build as realistic models as possible, we require *ex-ante* information on the underlying price drivers. More market-specifically, and in light of the design of intraday electricity markets, forecast errors of renewable power production have to be taken into account. Kiesel and Paraschiv (2017) deliver the first and only work fulfilling these prerequisites. Our article builds upon their work and develops an econometric price model with fundamental impacts for continuous intraday markets of 15-minute contracts.

Our main modeling assumption is that the price formation process on the intraday electricity market depends on the slope of the merit order curve. Figure 1 illustrates a merit order curve with and without the infeed from renewable energy sources (RES). The merit order curve is a non-linear and convex function of the marginal costs of power plants depending on the generation capacity. Equivalently, since the marginal costs of the last running power plant needed to cover demand set the final electricity price, the merit order curve may be interpreted as a function of the electricity price depending on the electricity demand, too.

Let us consider the merit order curve without renewable power infeed (blue solid). When there is low demand, only relatively cheap power generation technologies such as lignite-fired power plants are needed, whereas if demand is high, more expensive technologies such as gas-fired power plants might be required to satisfy demand. As exhibited in Figure 1, if demand is low, the slope of the merit order curve is relatively small and we call the market to be in a flat merit-order regime; however, if demand is high, the merit-order-curve slope is comparatively large and the market is said to be in a steep merit-order regime.

Let us turn towards the merit order curve with renewable power infeed (green dash-dotted). Since renewable energy sources have zero marginal costs, their infeed shifts the entire merit order curve to the right. As a consequence, if demand is low (flat regime), the electricity price decreases by a small amount ΔP_f; however, if demand is high (steep regime), the electricity price decreases as well but by a much larger amount $\Delta P_s > \Delta P_f$. We take into account this asymmetric effect of renewable power infeed on electricity prices in our econometric model by incorporating the slope of the merit order curve.

To model the merit order curve, two approaches have been proposed in the academic literature. The first approach models the merit order curve from the supply side via generation capacities and marginal costs of power plants. While generation capacities are given by market transparency data, one has to specify a model for the marginal costs of power plants. Pape et al. (2016); Kallabis et al. (2016); Beran et al. (2019) model the marginal costs as a function of fuel prices, CO_2 emission allowances prices, emission intensities of fuel types, power plant heat rates or thermal efficiencies, and other variable costs. As marginal costs depend on a wide variety of factors, this approach is highly complex and subject to strong modeling assumptions.

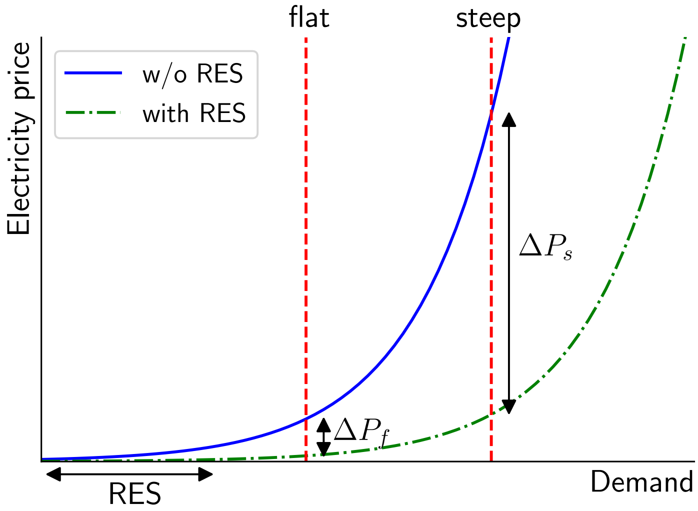

Figure 1: Merit order curve without (blue solid) and with (green dash-dotted) infeed from renewable energy sources (RES) indicating a flat and steep merit-order regime (red) with electricity price changes ΔP_f and ΔP_s, respectively.

The second approach models the merit order curve from the demand side via electricity loads, or load forecasts, and electricity prices as proposed by Burger et al. (2004); He et al. (2013). While electricity load is an indicator of total electricity demand, electricity prices are determined by the marginal costs of the price-setting power plant (marginal power plant). As data for both electricity loads and prices exist, this approach does not rely on modeling assumptions. Therefore, we follow the demand-side approach.

The intraday electricity market of 15-minute contracts has only recently come into focus of scientific research. To the best of our knowledge, only three studies exist hitherto. Kiesel and Paraschiv (2017) provide the first econometric model for 15-minute intraday prices. They model both deviations between day-ahead and last intraday prices as well as continuous intraday prices in a threshold regression context. They provide evidence that 15-minute prices respond asymmetrically to intradaily updated renewable forecast errors depending on the proportion of expected demand covered by conventional energy sources. Märkle-Huß et al. (2018) study how the introduction of 15-minute contracts has affected the day-ahead and intraday market of hourly contracts. They find that prices of hourly contracts decreased and trading volumes increased. Kath and Ziel (2018) present the first forecasting study of 15-minute prices using an elastic net regression model. They conclude that prices in the intraday auction are much easier to forecast than prices in the continuous trading.

This article extends the existing literature along a number of dimensions: First, we explore a novel and unique data set of high-frequency transaction data and linked fundamental supply and demand data. Intradaily updated forecasts of renewable power generation (solar, wind) constitute the heart of our data collection. These are the same real-time renewable forecasts as available to traders on the intraday market. As such, this is the most extensive data set used in the empirical literature to study the price formation process on intraday electricity markets. Hence, our data set allows for a more realistic model specification than proposed in previous research.

Second, we suggest the first econometric price model for 15-minute contracts that incorporates the slope of the merit order curve. This is a substantial improvement over Kiesel and Paraschiv (2017) as electricity prices react asymmetrically to renewable forecast changes depending on the merit-order-curve slope: If the merit order is steep, electricity prices change more severely in the wake of renewable forecast errors than if the merit order is flat. Moreover, our econometric model solely involves *ex-ante* market knowledge.

Third, and to the best of our knowledge, this is the first work studying the influence of neighboring 15-minute contracts on the price dynamics of a given contract. This is motivated by the fact that adjacent contracts are driven by similar market information.

This paper is organized as follows: In Section 2, we lay out our data set and perform an empirical analysis of intraday transaction data of 15-minute contracts. In Section 3, we present the existing econometric model by Kiesel and Paraschiv (2017) and our extended version of the model as well as the threshold regression. In Section 4, we calibrate the econometric models to market data and discuss our estimation results. We offer our conclusions in Section 5.

2 Stylized facts

In this section, we lay out our data set and perform an empirical analysis of the hourly seasonality and liquidity evolution of 15-minute contracts.

2.1 Data

We investigate high-frequency trade and linked fundamental data of all 96 15-minute contracts traded on the German continuous intraday power market at EPEX SPOT SE. Our observation period spans from January 1 to December 31, 2015. The trade data of 15-minute contracts involve transaction prices and trading volumes from the continuous intraday trading session with a 1-minute time resolution and are provided by European Energy Exchange AG (2016c). This, however, does not imply that we observe one transaction every minute, but it may take a multiple of one minute until the subsequent transaction is observed. In case of multiple transactions within the same trading minute, we compute the volume-weighted average price for that minute. The continuous trading session for 15-minute contracts opens daily at 4 PM and, in 2015, ends 45 and 30 minutes before delivery begins, respectively[1,2]. Furthermore, we use market clearing prices of 15-minute contracts traded in the German 15-minute intraday auction at EPEX SPOT SE, which takes place daily at 3 PM, provided by European Energy Exchange AG (2016b). The auction data may also be obtained via the `R` package `emarketcrawlR` by Wagner (2018). We shall denote a 15-minute contract by HhQq with $h = 0, \ldots, 23$ and $q = 1, \ldots, 4$; e.g., contract H13Q1 refers to the delivery period 1:00–1:15 PM.

As fundamental data, we include intraday wind and solar power forecasts, expected demand and expected conventional capacity. The intraday renewable power forecasts involve intradaily updated forecasts of wind and solar power production in Germany, which are the same real-time renewable forecasts as available to traders on the intraday market. These forecasts are updated every 15 minutes, where each update contains a forecast time series for the following eight days in a 15-minute time resolution, provided by EWE TRADING GmbH (2016). As such, the intraday renewable power forecasts constitute a unique data set and, to the best of our knowledge, have solely been analyzed by Kiesel and Paraschiv (2017). As an indicator of expected electricity demand, we use the day-ahead total load forecast for each quarter-hour on the following day in Germany, which is published daily at 10 AM and is provided by European Network of Transmission System Operators for Electricity Transparency Platform (2016). The expected conventional capacity covers the expected daily average of available generation capacity of conventional power plants on the following day in Germany, which is published daily at 10 AM and is provided by European Energy Exchange AG Transparency Platform (2016). As

[1]EPEX SPOT SE reduced the lead time on the German continuous intraday power market for hourly and 15-minute contracts from 45 to 30 minutes before delivery on July 16, 2015 (EPEX SPOT SE, 2015).

[2]On June 14, 2017, the lead time within the four German control zones was locally further reduced to 5 minutes before delivery (EPEX SPOT SE, 2017).

conventional energy sources, we include coal, garbage, gas, lignite, oil, other, pumped-storage, run-of-the-river, seasonal-store, uranium. A summary of the employed data may be found in Table A.1 in Appendix A.

2.2 Hourly seasonality

2.2.1 Transaction prices

Figure 2 illustrates the volume-weighted average transaction price of 15-minute contracts during peak hours and off-peak hours for summer and winter. We identify an hourly seasonality of volume-weighted average prices for both peak and off-peak hours as well as for summer and winter[3]. The hourly seasonality exhibits a sawtooth-like shape: For the peak-hour contracts H8Q1–H13Q4, the average price of the first 15-minute contract within each hour is the highest and it declines until the last 15-minute contract within that hour, which has the lowest average price. Conversely, for contracts H14Q1–H18Q4, the lowest average price is present for the first 15-minute contract which increases up to the highest average price for the last 15-minute contract in a given hour.

The hourly seasonality pattern and its change around noon may be explained by electricity generation from solar energy: In the first half of the day, the sun rises and less electricity from solar energy is produced during the first quarter-hour as compared to the last quarter-hour within each hour. If a (renewable) electricity supplier sold an hourly contract on the day-ahead market, it has to buy electricity for the first quarter-hour on the intraday market to meet its obligation since less electricity is produced from solar energy than it has sold (buy pressure); thus prices increase. In the last quarter-hour, however, more solar electricity is generated than it has sold on the day-ahead market and so it wants to sell the surplus on the intraday market to avoid entering the balancing energy market (sell pressure); hence prices decrease. In the second half of the day, after the sun has reached its highest level (around 2 PM in Germany), more solar power is generated during the first than in the last quarter-hour in each hour. Thus, there is a sell pressure in the first and a buy pressure in the last quarter-hour of an hour, and the pattern is reversed. The existence of buy and sell pressure is underpinned by the hourly seasonality of trading volumes described in Section 2.2.2.

Similarly, the sawtooth-shaped hourly seasonality of volume-weighted average prices is found during off-peak hours. For contracts H20Q1–H1Q4, the average price of the first and last quarter-hourly contract within an hour is highest and lowest, respectively, while for contracts H4Q1–H6Q4, this is reversed. The hourly seasonality at night stems from the design of conventional power plants which ramp up and down.

Overall, during peak hours, average transaction prices are lower in summer than in winter apart from a few exceptions. In the afternoon and evening hours, that is, for contracts H14Q1–H19Q4, we find larger deviations between summer and winter average prices than in morning and noon hours. During off-peak hours, average prices are fairly similar during both seasons most of the time and only slightly lower in winter than in summer.

2.2.2 Trading volumes

Figure 3 shows the total trading volume of 15-minute contracts during peak hours and off-peak hours averaged over the year. We only present the yearly average of total trading volumes as the distinction between summer and winter does not provide additional information. Similar to transaction prices, we observe an hourly seasonality of total trading volumes for both peak and off-peak hours. The hourly seasonality of trading volumes has a U-shape: Larger total trading volumes are found for the first and last 15-minute contract within each hour of the

[3]The hourly seasonality preserves for unweighted average transaction prices both qualitatively and quantitatively: The seasonal averages of unweighted and volume-weighted average prices differ by roughly 2% only.

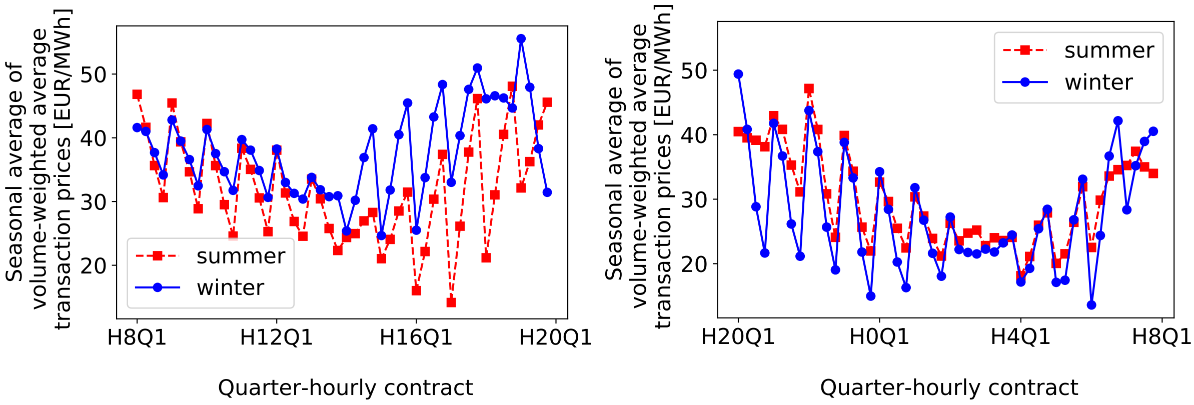

Figure 2: Volume-weighted average transaction price of 15-minute contracts during peak hours (left) and off-peak hours (right) averaged over summer (red) and winter (blue).

day, while the second and third 15-minute contract in an hour always exhibit lower trading volumes. More specifically, the last 15-minute contract entails the largest trading volume, while the second 15-minute contract involves the lowest trading volume in an hour. The U-shaped hourly seasonality supports our hypothesis of buy and sell pressure for the marketing of solar power in the first and last quarter-hour during peak hours, respectively.

15-minute contracts during off-peak hours are generally associated with less trading volume than peak-hour contracts. Total trading volumes are particularly low for contracts H0Q1–H5Q4. However, the U-shaped hourly seasonality of trading volumes is persistent during off-peak hours. The hourly seasonality at night results from balancing out the ramp-up and -down of conventional power plants.

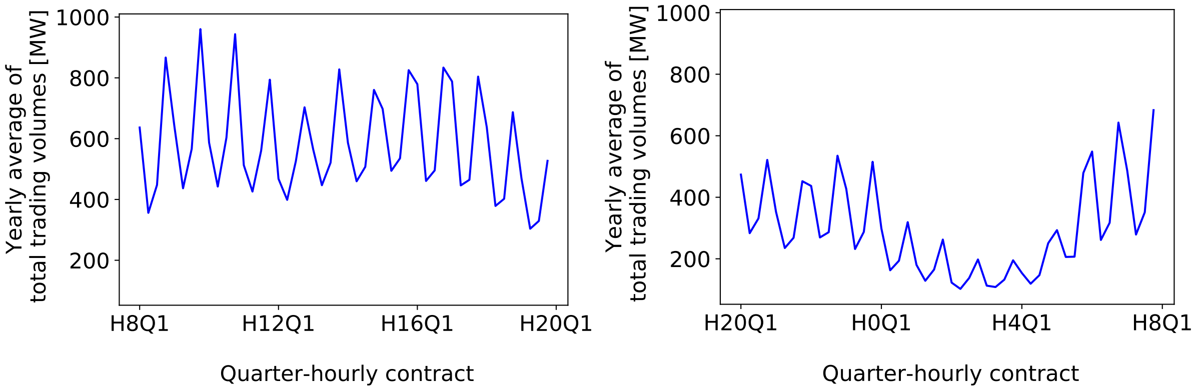

Figure 3: Total trading volume of 15-minute contracts during peak hours (left) and off-peak hours (right) averaged over the year.

2.3 Liquidity evolution

2.3.1 Gate closure

Figure 4 displays the temporal evolution of liquidity of 15-minute contracts over the trading session towards gate closure. As measures for market liquidity, we use the number of trades and total trading volume aggregated over all 15-minute contracts and all trading sessions. Due to low liquidity far from gate closure, we focus on the last three trading hours prior to gate closure. We note that EPEX SPOT SE reduced the lead time on the German intraday power market for hourly and 15-minute contracts from 45 to 30 minutes before delivery on July 16, 2015 (EPEX SPOT SE, 2015). Thus, to avoid effects due to the shift of lead time, we synchronize our trade time series with respect to gate closure by shifting the trade time stamps of 15-minute contracts maturing before July 16, 2015 by 15 minutes.

The number of trades increases from 952 three hours to gate closure to 3,054 one hour to gate closure. Subsequently the number of trades rises further and more than doubles to 7,080 half an hour to gate closure. 15 minutes to gate closure, the number of trades jumps to 16,593 while 13 minutes before gate closure it reaches a local maximum of 28,378. The surge of trading activity around 15 minutes to gate closure may be associated with the fact that a given contract becomes the front 15-minute contract. The maximum value of 30,512 trades is observed one minute to gate closure.

The total trading volume increases from 12 GW to 48 GW between three and one hour to gate closure. Thereafter, trading volume almost triples to 135 GW half an hour to gate closure. 15 and 13 minutes before gate closure, total trading volume raises to 261 GW and 314 GW, respectively, which coincides with becoming the front 15-minute contract. A comparison with the number of trades at these points in time in Figure 4 reveals that indeed a vast number of transactions is executed but with comparatively low trading volumes. The total trading volume peaks at 960 GW one minute to gate closure.

Thus, we observe that liquidity of 15-minute contracts rises severely within the last trading hour prior to gate closure: On average, roughly 68% of the number of transactions are executed and roughly 74% of the total trading volume is transferred. The reason why the majority of trading takes place close to gate closure is that forecasts of fundamentals, particularly renewable power forecasts, become more and more precise regarding the delivery period of a given 15-minute contract. Hence, it is desirable to trade as closest to delivery begin as possible. Glas et al. (2020); Graf von Luckner and Kiesel (2020) document an increasing liquidity towards gate closure for hourly contracts on the German intraday electricity market, too.

We identify a small but distinct rise in liquidity every 15 minutes. This is particularly pronounced for the number of trades but present for the total trading volume, too. Consequently, an increased amount of transactions with relatively little trading volume is conducted periodically. We argue that the 15-minute periodicity in liquidity originates from newly arriving renewable forecast updates. As described in Section 2.1, renewable forecasts are updated in 15-minute intervals. New forecasts will not have changed much after 15 minutes and thus traders only make minor adjustments to their positions by trading little volume. Moreover, we observe that trading activity increases at isolated points in time and dies out immediately until the next increase. Therefore, we conclude that renewable forecast updates are reflected in prices of 15-minute contracts within one trading minute.

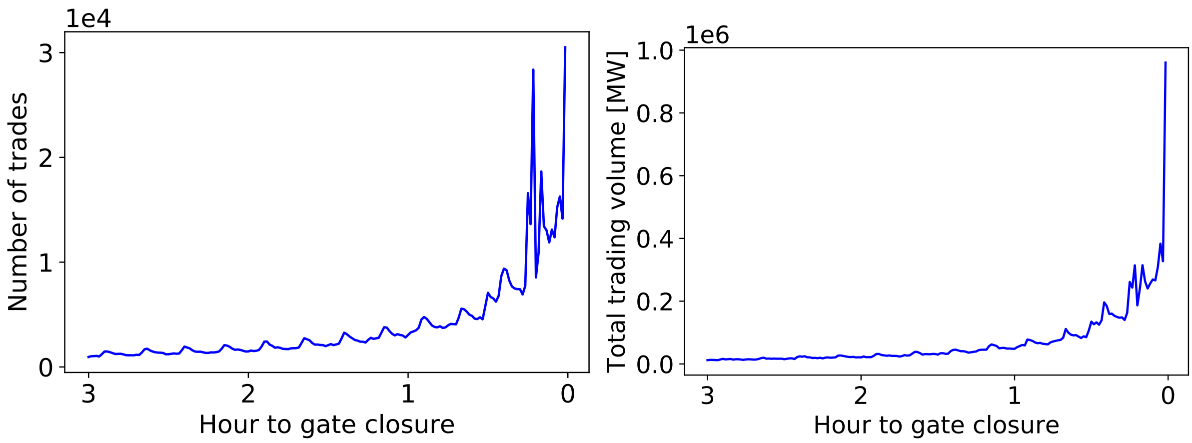

Figure 4: Time evolution of the number of trades (left) and total trading volume (right) through the trading session towards gate closure.

2.3.2 Gate opening

Figure 5 illustrates the temporal development of liquidity of 15-minute contracts after gate opening at 4 PM. The number of trades amounts to 4,718 just after gate opening and decreases to 705 12 minutes after gate opening. 15 minutes after gate opening, the number of trades reaches its maximum value of 5,309, which drains within the next trading minute. Similarly, liquidity jumps to 2,276 trades 30 minutes after gate opening and falls back to its prior level within two trading minutes. Thereafter, liquidity approaches a fairly stable level of 185 trades, on average, between one and two hours after gate opening.

The total trading volume peaks at 58 GW shortly after gate opening and steadily declines to 5.6 GW 12 minutes after gate opening. 15 minutes after gate opening, total trading volume rises to 13 GW while it amounts to 3.5 GW 30 minutes after gate opening. Comparing trading volume and the number of trades at these points in time shows that the surge in trading activity involves relatively little trading volume. Subsequently, the total trading volume keeps a quite constant and low level around 1.5 GW until two hours after gate opening.

Thus, liquidity of 15-minute contracts is high close to gate opening and drops substantially during the first 12 trading minutes. This behavior may be explained by the fact that market participants initialize their positions. In the sequel, little volume is traded and thereby only minor adjustments are made to the open positions. Generally, liquidity remains poor until the last trading hour prior to gate closure as the forecasts of fundamentals are still relatively inaccurate.

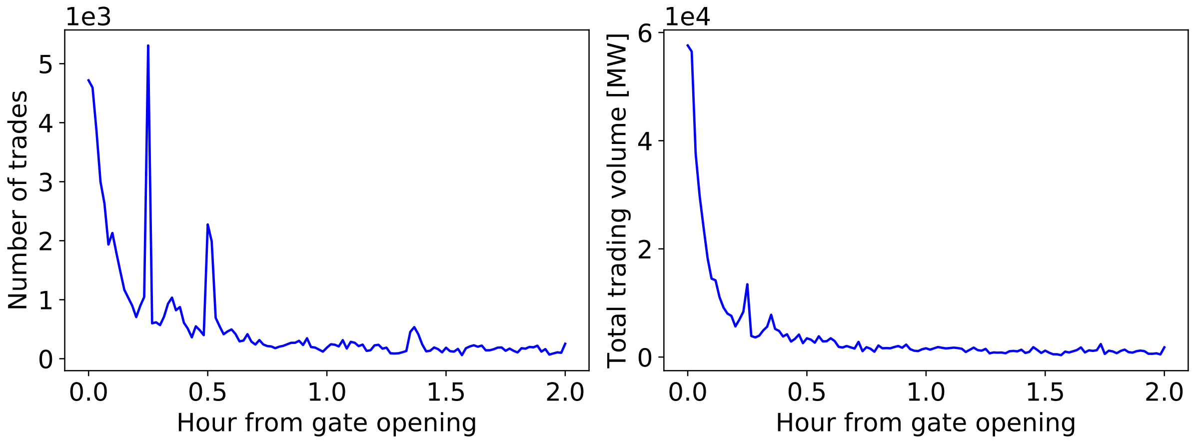

Figure 5: Time evolution of the number of trades (left) and total trading volume (right) after gate opening.

3 Methodology

We aim at modeling the asymmetric response of 15-minute intraday electricity prices to explanatory variables, in particular, to renewable forecast changes. As a starting point, we reimplement the econometric model by Kiesel and Paraschiv (2017). Moreover, we suggest an extension of their model to overcome its weaknesses. We employ a threshold regression model to calibrate the econometric models to market data.

3.1 Benchmark econometric model

We use the econometric model for intraday price changes of 15-minute contracts proposed by Kiesel and Paraschiv (2017) as a benchmark. For each 15-minute contract, the model specification reads

$$\Delta P_t = \alpha_0 + \sum_{\tau=1}^{3} \alpha_\tau \, \Delta P_{t-\tau} + \alpha_4 \, V_t + \alpha_5 \, DQ + \alpha_6 \, \Delta w_t^n + \alpha_7 \, \Delta w_t^p + \alpha_8 \, \Delta s_t^n + \alpha_9 \, \Delta s_t^p + \alpha_{10} \sqrt{\Delta t} + \epsilon_t \,, \tag{1}$$

where $\Delta P_t = P_t - P_{t-1}$ denotes the transaction price change between times t and $t-1$, V_t the trading volume at time t, $DQ = \frac{\ell}{c}$ the demand quota with expected demand ℓ and expected conventional capacity c for a given 15-minute contract, $\Delta w_t^n = \min(\Delta w_t, 0)$ and $\Delta w_t^p = \max(\Delta w_t, 0)$ negative and positive wind power forecast changes, respectively, where $\Delta w_t = w_t - w_{t-1}$ is the last available wind power forecast change at time t, $\Delta s_t^n = \min(\Delta s_t, 0)$ and $\Delta s_t^p = \max(\Delta s_t, 0)$ negative and positive solar power forecast changes, respectively, where $\Delta s_t = s_t - s_{t-1}$ is the last available solar power forecast change at time t, and Δt the interarrival time between two consecutive transactions conducted at times t and $t-1$.

The sum in Equation (1) covers three lagged price changes $\Delta P_{t-\tau}$, $\tau = 1, 2, 3$, that is, autoregressive terms, where the number of lags has been determined by partial autocorrelation of price changes. Moreover, we distinguish between positive and negative wind and solar power forecast errors $\Delta w_t^p, \Delta s_t^p$ and $\Delta w_t^n, \Delta s_t^n$, respectively, as we expect them to have opposite effects on electricity price changes ΔP_t: Positive renewable forecast errors should decrease electricity prices, whereas negative renewable forecast errors should increase electricity prices. We control for the interarrival time Δt since transactions do not take place at equidistant points in time, but it may take one minute or several hours until the next trade is conducted.

The demand quota DQ quantifies the proportion of expected demand l which is expected to be met by conventional power generation capacities c; or, put another way, how much the expected conventional capacity c does cover expected demand l. We use the demand quota DQ as threshold variable since we assume that the gap between expected demand l and expected conventional capacity c influences the trading behavior of market participants on the intraday market: A large gap induces a great necessity to balance electricity produced from renewable energy sources, whereas a small gap puts less pressure to adjust renewable electricity (see Kiesel and Paraschiv, 2017, chap. 2, for a more detailed discussion).

The demand quota DQ is the only variable remaining constant during the continuous trading session of a 15-minute contract. However, it does depend on the specific contract since the expected demand l is provided in quarter-hourly granularity. In particular, the value of DQ is known daily at 10 AM and thus before continuous trading begins. From a trader's perspective, the demand quota is well suited as threshold variable, too, since it indicates in which regime the market is before continuous trading begins. Thereby, the corresponding intraday price model can be chosen *ex-ante*.

3.2 Extended econometric model

We refine the econometric model by Kiesel and Paraschiv (2017) along three dimensions by incorporating supplementarily: (i) the slope of the merit order curve, (ii) price changes of neighboring 15-minute contracts, (iii) the 15-minute intraday auction price. For a given 15-minute contract $i = 1, \dots, 96$, the model specification reads

$$\Delta P_t^{(i)} = \alpha_0^{(i)} + \sum_{\tau=1}^{m} \alpha_\tau^{(i)} \Delta P_{t-\tau}^{(i)} + \sum_{\substack{j=-n, \\ j \neq 0}}^{n} \beta_j^{(i)} \Delta P_t^{(i+j)} + \eta_1^{(i)} \xi^{(i)} + \eta_2^{(i)} P^{\mathrm{Auc},(i)} + \eta_3^{(i)} V_t^{(i)} + \eta_4^{(i)} \Delta w_t^{n,(i)} + \eta_5^{(i)} \Delta w_t^{p,(i)} + \eta_6^{(i)} \Delta s_t^{n,(i)} + \eta_7^{(i)} \Delta s_t^{p,(i)} + \eta_8^{(i)} \sqrt{\Delta t^{(i)}} + \epsilon_t^{(i)} \,, \tag{2}$$

where $\Delta P_t^{(i+j)}$ denotes the last observed price change at time t of neighboring contract $i+j$, $\xi^{(i)}$ the slope of the merit order curve, and $P^{\mathrm{Auc},(i)}$ the 15-minute intraday auction price of contract i. The remaining variables correspond to the benchmark model (1) described in Section 3.1.

The first sum in Equation (2) covers m autoregressive price changes $\Delta P_{t-\tau}^{(i)}$, $\tau = 1, \ldots, m$. To determine the number of lags, we use the partial autocorrelation of price changes and choose $m = 3$. The second sum in Equation (2) captures the price change $\Delta P_t^{(i+j)}$, $j = -n, \ldots, n$, $j \neq 0$, at time t of n 15-minute contracts maturing before and n 15-minute contracts maturing after contract i. For example, if $n = 2$ and $i =$ H13Q1, the price change at time t of contracts H12Q3, H12Q4, H13Q2, H13Q3 is included. The intraday auction price $P^{\mathrm{Auc},(i)}$ remains constant during the trading session of a given contract i and can be considered as an estimate of the initial price of contract i in the continuous trading.

We use the slope of the merit order curve $\xi^{(i)}$ as threshold variable instead of the demand quota DQ compared to Kiesel and Paraschiv (2017). One weakness of the demand quota DQ is that it does not recognize whether the market is in a flat or steep merit-order-curve regime: Proportionally speaking, a high expected demand l and high expected conventional capacity c lead to the same value of DQ as low demand and low capacity. Another weakness is that the demand quota aggregates expected capacities over all conventional generation technologies. Thus, it loses information on the price-setting power plant and the slope of the merit order curve. We overcome these limitations in our extended econometric model (2).

We estimate $\xi^{(i)}$ from empirical intraday auction prices $P^{\mathrm{Auc},(i)}$ and expected demands, or total load forecasts, $\ell^{(i)}$ in the spirit of Burger et al. (2004); He et al. (2013). This approach is reasonable for describing the slope of the merit order curve since the level of intraday auction prices reflects the marginal costs of power plants needed to cover expected demand. Burger et al. (2004); He et al. (2013) construct a merit order curve for the electricity spot market as a whole, independent of the contract, from hourly day-ahead prices and hourly load forecasts. We, however, determine a merit order curve for each 15-minute contract i individually and thus arrive at a more fine-grained picture. We fit a function $f(\ell)$ to the price–load data and call $f(\ell)$ the empirical merit order curve[4]. Then we take the derivative of the empirical merit order curve $f'(\ell) = \frac{\mathrm{d}f(\ell)}{\mathrm{d}\ell}$ and substitute empirical expected demands $\ell^{(i)}$ into $f'(\ell)$ to obtain empirical merit-order-curve slopes $\xi^{(i)} = f'\left(\ell^{(i)}\right)$.

The slope of the merit order curve $\xi^{(i)}$ remains constant during the trading session of contract i. The value of $\xi^{(i)}$ can be determined daily around 3:10 PM, after the publication of the intraday auction results, and hence before continuous trading begins. Thus, $\xi^{(i)}$ indicates whether the market is in a flat or steep merit-order regime *ex-ante* and the appropriate intraday price model can be chosen accordingly. This is an attractive feature of our econometric model for practical applications.

3.3 Threshold regression

We use the threshold regression model introduced by Hansen (2000) to calibrate our econometric models to market data. The threshold regression model is able to reveal asymmetries in the impact of explanatory variables with respect to a specified threshold variable. The basic concept of the threshold regression involves two steps: First, the entire sample is split into two subsamples, also referred to as groups, classes, or regimes, at a certain threshold value of a designated threshold variable; second, a linear regression model is estimated on each subsample separately.

More formally, suppose we observe the sample $\{y_i, \mathbf{x}_i, q_i\}_{i=1}^n$, where y_i is the dependent variable, $\mathbf{x}_i \in \mathbb{R}^m$ collects the independent variables, and q_i denotes the threshold variable. The threshold variable q_i may be one of the independent variables gathered in $\mathbf{x}_i$ and must have a

[4]Burger et al. (2004) call f empirical price load curve.

continuous distribution. The threshold regression model reads

$$\begin{aligned} y_i &= \begin{cases} \boldsymbol{\theta}_1' \, \mathbf{x}_i + \varepsilon_i, & \text{if } q_i \le \gamma \\ \boldsymbol{\theta}_2' \, \mathbf{x}_i + \varepsilon_i, & \text{if } q_i > \gamma \end{cases}, \\ &= \boldsymbol{\theta}_1' \, \mathbf{x}_i \, \mathbb{1}\{q_i \le \gamma\} + \boldsymbol{\theta}_2' \, \mathbf{x}_i \, \mathbb{1}\{q_i > \gamma\} + \varepsilon_i \,, \qquad i = 1, \dots, n, \end{aligned} \tag{3}$$

where γ is the threshold parameter, $\boldsymbol{\theta}_1, \boldsymbol{\theta}_2 \in \mathbb{R}^m$ collect the regression parameters, $\mathbb{1}$ denotes the indicator function, and ε_i is the error term. Thus, the observed sample is split into two subsamples along the threshold variable q_i at a specific value γ. By design, the threshold regression model (3) allows the regression parameters in $\boldsymbol{\theta}_1, \boldsymbol{\theta}_2$ to vary between the regimes.

In order to estimate the threshold regression model, we reformulate Equation (3): Let $\mathbf{x}_i(\gamma) = \mathbf{x}_i \, \mathbb{1}\{q_i \le \gamma\}$ and call $\boldsymbol{\delta}_n = \boldsymbol{\theta}_1 - \boldsymbol{\theta}_2$ the threshold effect. Then the threshold model (3) can be written in the alternative form,

$$y_i = \boldsymbol{\theta}' \mathbf{x}_i + \boldsymbol{\delta}_n' \, \mathbf{x}_i(\gamma) + \varepsilon_i \,, \qquad i = 1, \dots, n, \tag{4}$$

where $\boldsymbol{\theta} = \boldsymbol{\theta}_2$. Stacking the variables y_i and ϵ_i results in vectors $\mathbf{y}, \boldsymbol{\varepsilon} \in \mathbb{R}^n$, and stacking the vectors $\mathbf{x}_i'$ and $\mathbf{x}_i(\gamma)'$ yields matrices $\mathbf{X}, \mathbf{X}_\gamma \in \mathbb{R}^{n \times m}$. Then Equation (4) can be expressed in matrix notation,

$$\mathbf{y} = \mathbf{X} \, \boldsymbol{\theta} + \mathbf{X}_\gamma \, \boldsymbol{\delta}_n + \boldsymbol{\varepsilon} \,, \tag{5}$$

where $\boldsymbol{\theta}, \boldsymbol{\delta}_n, \gamma$ are the regression parameters which can be estimated by least squares. By definition, the least squares estimates $\hat{\boldsymbol{\theta}}, \hat{\boldsymbol{\delta}}, \hat{\gamma}$ jointly minimize the sum of squared errors function,

$$S_n(\boldsymbol{\theta}, \boldsymbol{\delta}, \gamma) = (\mathbf{y} - \mathbf{X} \, \boldsymbol{\theta} - \mathbf{X}_\gamma \, \boldsymbol{\delta})' \, (\mathbf{y} - \mathbf{X} \, \boldsymbol{\theta} - \mathbf{X}_\gamma \, \boldsymbol{\delta}) \,. \tag{6}$$

The threshold parameter estimate $\hat{\gamma}$ may be obtained by minimizing the concentrated sum of squared errors function $S_n(\gamma)$,

$$\hat{\gamma} = \arg\min_\gamma S_n(\gamma) \,, \tag{7}$$

where

$$S_n(\gamma) = \mathbf{y}'\mathbf{y} - \mathbf{y}'\mathbf{X}_\gamma^* \, (\mathbf{X}_\gamma^{*\prime}\mathbf{X}_\gamma^*)^{-1} \mathbf{X}_\gamma^{*\prime} \, \mathbf{y} \,, \tag{8}$$

and $\mathbf{X}_\gamma^* = [\mathbf{X} \, \mathbf{X}_\gamma]$. Given the threshold estimate $\hat{\gamma}$, the regression parameter estimates $\hat{\boldsymbol{\theta}} = \hat{\boldsymbol{\theta}}(\hat{\gamma})$ and $\hat{\boldsymbol{\delta}} = \hat{\boldsymbol{\delta}}(\hat{\gamma})$ arise from ordinary least squares regression of $\mathbf{y}$ on $\mathbf{X}_\gamma^*$.

To test the hypothesis $H_0 : \gamma = \gamma_0$, the likelihood ratio statistic,

$$LR_n(\gamma) = n \, \frac{S_n(\gamma) - S_n(\hat{\gamma})}{S_n(\hat{\gamma})} \,, \tag{9}$$

is used under the auxiliary assumption $\varepsilon_i \overset{\text{iid}}{\sim} \mathcal{N}(0, \sigma^2)$. We reject the likelihood ratio test of H_0 for large values of $LR_n(\gamma_0)$. Asymptotic p-values for the likelihood ratio test can then be computed by

$$p_n = 1 - \left(1 - \mathrm{e}^{-\frac{1}{2} \, LR_n(\gamma_0)^2}\right)^2 . \tag{10}$$

We employ the R package `thrreg` developed by Kremer (2020) to estimate the threshold regression model.

4 Estimation results

4.1 Benchmark econometric model

We estimate the parameters of the benchmark econometric model (1) by Kiesel and Paraschiv (2017) by the threshold regression described in Section 3.3 for all 96 15-minute contracts. Here, a selection of 15-minute contracts representative for morning, noon, and evening hours is analyzed, that is, H7, H13, H18, Q1–Q4 each. We compare our estimation results stemming from January–December 2015 data with the results by Kiesel and Paraschiv (2017), who study January–June 2014 data. For all contracts, we use the demand quota DQ as threshold variable.

The estimation results of all 15-minute contracts in hours H13, H7, H18 are presented in Tables 1, 2, 3, respectively. The threshold test reveals strong evidence for a threshold effect in the demand quota DQ for all contracts in hours H13 and H7, while in hour H18, it suggests a statistically significant threshold effect for contract Q2 only[5]. The estimated threshold parameter amounts to $\hat{\gamma} \approx 1.1$ for all contracts. A demand quota of $DQ = 1.1$ implies that the expected total electricity demand l exceeds expected conventional capacity c by approximately 10%. Likewise this value implies that roughly 10% renewable power infeed is expected. In general, the low demand quota regime (Regime 1) describes a market in which much conventional power generation is planned to meet expected demand, since little renewable power production is anticipated. Conversely, the market is in the high demand quota regime (Regime 2) if much renewable power infeed is anticipated and consequently less conventional power generation is planned. For all contracts, the total sample is split into subsamples of reasonable size and allows for a sound interpretation of the estimation results. The adjusted R^2 ranges between 9% and 21%.

The estimated coefficients of lagged price changes $\Delta P_{t-1}, \Delta P_{t-2}$ are highly statistically significant and negative in both regimes for all contracts, and even the coefficients of ΔP_{t-3} are significant and negative in most cases. For evening contracts, the higher-order autoregressive terms lose statistical significance. The negative coefficients of lagged price changes are an indicator of mean reversion in the price formation process of 15-minute contracts. As such, they reflect the so-called "learning effect" or "participant conduct" (Karakatsani and Bunn, 2010; Frauendorfer et al., 2018). Our results confirm previous findings of Kiesel and Paraschiv (2017) for morning and evening contracts. For noon contracts, in contrast, they find that autoregressive terms have less explanatory power and intraday trading is primarily driven by renewable forecast changes. Our results, however, suggest that autoregressive terms and the mean reversion pattern associated therewith play an essential role for intraday trading at noon in 2015.

The estimated coefficients of trading volume V_t are statistically significant for most of the contracts and regimes. For contracts H13Q1 and H13Q2, they are negative, whereas for H13Q3 and H13Q4, they turn positive independent of the regime. The same sign profile is found for contracts H18Q1 and H18Q4. This sign pattern is reasonable as it reflects the joint hourly seasonality of transaction prices and trading volumes described in Section 2.2: In the first half of an hour, more solar power is produced than the hourly average which induces sell pressure and thus electricity prices decrease; in the second half of an hour, less solar power is generated than the hourly average leading to buy pressure and electricity prices increase. In morning hours, we observe the opposite: For contracts H7Q1 and H7Q2, the coefficients of V_t are positive, whereas for H7Q3 and H7Q4, they turn negative independent of the regime. This sign pattern coincides with buy and sell pressure at the beginning and end of the hour, respectively. Overall, we find an asymmetric response of intraday price changes ΔP_t to trading volumes V_t. This confirms the results of Kiesel and Paraschiv (2017).

In hour H13, the coefficients of negative wind forecast changes Δw_t^n are statistically significant and negative in both regimes for all contracts, whereas coefficients of positive wind forecast

[5]We indicate the statistical significance level of the threshold test by superscript asterisks at the threshold variable in the regression tables.

changes Δw_t^p are not significant. In Kiesel and Paraschiv (2017), the coefficients of Δw_t^n and Δw_t^p are also negative but only significant in the high demand quota regime. In hour H7, the coefficients of negative wind forecast changes Δw_t^n are significant and negative in the high demand quota regime for Q1–Q3, whereas coefficients of positive wind forecast changes Δw_t^p are significant and negative for Q1 and Q2. In Kiesel and Paraschiv (2017), the coefficients of Δw_t^n are not significant, while some coefficients of Δw_t^p are significant but with no clear regularity. In hour H18, the coefficients of negative and positive wind forecast changes Δw_t^n, Δw_t^p are rarely significant and mostly negative. This is in line with Kiesel and Paraschiv (2017). The negative coefficients of Δw_t^n, Δw_t^p are economically meaningful and reflect rising and falling electricity prices as a result of less and more wind power infeed, respectively. Overall, no asymmetry in the coefficients of wind forecast changes between the regimes is found. We conclude that forecast errors of wind power generation contribute to pricing electricity for noon and morning contracts, but they are less significant for pricing evening contracts.

In hours H13 and H7, the coefficients of negative solar forecast changes Δs_t^n are significant and negative in the high demand quota regime, but never significant in the low regime for all contracts. In hour H18, the coefficients of Δs_t^n are generally not significant. The coefficients' negative sign is reasonable as electricity prices should increase if less solar power is forecasted. In Kiesel and Paraschiv (2017), the coefficients of Δs_t^n are also negative in the high regimes but only significant for some contracts. In the high demand quota regimes, the coefficients of Δs_t^n are at least three times larger by absolute value than in the low regimes. The high regime implies that much renewable power infeed is expected; if solar forecast changes are negative, they contradict our expectation of the electricity generation mix established day-ahead and thus influence electricity prices more severely than in the low regime. In Kiesel and Paraschiv (2017), this asymmetry is less or not at all pronounced.

The coefficients of positive solar forecast changes Δs_t^p are significant and negative in both regimes for contracts H13Q1–Q3, while in hours H7 and H18, the coefficients of Δs_t^p are rarely significant and mostly negative. The negative sign is intuitive and illustrates that a larger expectation of solar power infeed decreases electricity prices. In the low demand quota regimes in hour H13, the coefficients of Δs_t^p are two to four times larger than in the high regimes. The low regime implies that little renewable power production is anticipated; it is reasonable that positive solar forecast changes in the low regime decrease electricity prices more severely than in the high regime where more renewable power infeed is planned anyway. Our results confirm the findings of Kiesel and Paraschiv (2017).

Eventually, intraday price changes of 15-minute contracts are driven by both autoregressive terms and fundamental variables at noon. In morning and evening hours, however, intraday trading is primarily affected by lagged price changes.

4.2 Extended econometric model

We estimate the parameters of the extended econometric model (2) by the threshold regression described in Section 3.3 for all 96 15-minute contracts. As representatives of morning, noon, and evening hours, we exemplarily analyze 15-minute contracts H7, H13, H18, Q1–Q4 each. For all contracts, the merit-order-curve slope ξ is used as threshold variable.

4.2.1 Merit-order-curve slope

We estimate the slope of the merit order curve $\xi^{(i)}$ of 15-minute contract i based on intraday auction prices $P^{\mathrm{Auc},(i)}$ and corresponding expected demands $\ell^{(i)}$. As both $P^{\mathrm{Auc},(i)}$ and $\ell^{(i)}$ are provided in quarter-hourly resolution, we are able to determine a merit order curve for each 15-minute contract i individually. Figure 6 depicts a scatter plot of empirical intraday auction prices $P_d^{\mathrm{Auc},(i)}$ versus empirical expected demands $\ell_d^{(i)}$ observed on days $d = 1, \ldots, T$, for contract $i =$ H13Q4. We filter out a total of 13 negative auction prices. We observe a

	H13Q1			
	Regime 1		Regime 2	
	$DQ^{***} \le 1.100$		$DQ^{***} > 1.100$	
Variable	Estimate	Std error	Estimate	Std error
Const	−1.337	(0.990)	−0.391	(1.725)
DQ	1.466	(0.977)	0.361	(1.464)
ΔP_{t-1}	−0.318***	(0.026)	−0.269***	(0.024)
ΔP_{t-2}	−0.151***	(0.021)	−0.072***	(0.018)
ΔP_{t-3}	−0.093***	(0.025)	−0.059**	(0.019)
V_t	−0.022***	(0.004)	−0.014***	(0.004)
Δw_t^n	−1.137***	(0.322)	−1.180***	(0.260)
Δw_t^p	−0.796*	(0.332)	−0.587	(0.303)
Δs_t^n	0.111	(0.428)	−1.730***	(0.534)
Δs_t^p	−3.545***	(0.492)	−1.374***	(0.428)
Δt	0.092***	(0.020)	0.061***	(0.021)
#Obs	6499		6554	
R^2_{adj}	0.158		0.143	

	H13Q2			
	Regime 1		Regime 2	
	$DQ^{***} \le 1.065$		$DQ^{***} > 1.065$	
Variable	Estimate	Std error	Estimate	Std error
Const	−1.403	(1.534)	−1.765	(1.455)
DQ	1.600	(1.574)	1.442	(1.239)
ΔP_{t-1}	−0.281***	(0.028)	−0.304***	(0.029)
ΔP_{t-2}	−0.142***	(0.024)	−0.093***	(0.019)
ΔP_{t-3}	−0.047*	(0.025)	0.014	(0.030)
V_t	−0.022***	(0.007)	−0.005	(0.008)
Δw_t^n	−1.300***	(0.351)	−1.175***	(0.245)
Δw_t^p	−0.606	(0.378)	−0.220	(0.208)
Δs_t^n	−0.390	(0.552)	−1.738***	(0.385)
Δs_t^p	−3.442***	(0.432)	−1.329**	(0.438)
Δt	0.053	(0.026)	0.035	(0.019)
#Obs	4279		7764	
R^2_{adj}	0.121		0.136	

	H13Q3			
	Regime 1		Regime 2	
	$DQ^{*} \le 1.019$		$DQ^{*} > 1.019$	
Variable	Estimate	Std error	Estimate	Std error
Const	0.574	(1.825)	−2.007	(1.175)
DQ	−0.877	(1.950)	1.507	(1.023)
ΔP_{t-1}	−0.270***	(0.028)	−0.269***	(0.021)
ΔP_{t-2}	−0.116***	(0.030)	−0.138	(0.019)
ΔP_{t-3}	−0.027	(0.023)	−0.073	(0.016)
V_t	0.014*	(0.008)	0.012	(0.004)
Δw_t^n	−0.892*	(0.479)	−1.125	(0.254)
Δw_t^p	−0.134	(0.318)	−0.522	(0.219)
Δs_t^n	0.204	(0.449)	−2.063***	(0.446)
Δs_t^p	−2.292***	(0.518)	−1.267	(0.461)
Δt	−0.023	(0.028)	0.026	(0.019)
#Obs	3538		9278	
R^2_{adj}	0.085		0.125	

	H13Q4			
	Regime 1		Regime 2	
	$DQ^{***} \le 1.148$		$DQ^{***} > 1.148$	
Variable	Estimate	Std error	Estimate	Std error
Const	−2.969	(0.712)	−4.635	(2.765)
DQ	2.609	(0.671)	3.765	(2.299)
ΔP_{t-1}	−0.292***	(0.021)	−0.219***	(0.023)
ΔP_{t-2}	−0.128***	(0.015)	−0.102***	(0.021)
ΔP_{t-3}	−0.049***	(0.014)	−0.094***	(0.020)
V_t	0.014**	(0.003)	0.007	(0.003)
Δw_t^n	−1.527***	(0.298)	−1.203***	(0.313)
Δw_t^p	−0.355	(0.220)	−0.299	(0.443)
Δs_t^n	−0.811	(0.333)	−3.001***	(0.684)
Δs_t^p	−0.450	(0.498)	−1.779	(0.696)
Δt	−0.036	(0.020)	−0.025	(0.027)
#Obs	10 372		4782	
R^2_{adj}	0.110		0.148	

$^{*}p < 0.1$; $^{**}p < 0.05$; $^{***}p < 0.01$

Table 1: Estimation results of the benchmark econometric model (1) for intraday price changes ΔP_t of 15-minute contracts H13Q1–4.

	H7Q1			
	Regime 1		Regime 2	
	$DQ^{***} \leq 1.022$		$DQ^{***} > 1.022$	
Variable	Estimate	Std error	Estimate	Std error
Const	1.277	(1.613)	−0.575	(2.142)
DQ	−2.147	(1.833)	−0.379	(1.896)
ΔP_{t-1}	−0.332***	(0.031)	−0.375***	(0.025)
ΔP_{t-2}	−0.148***	(0.031)	−0.169***	(0.021)
ΔP_{t-3}	−0.087***	(0.028)	−0.063***	(0.018)
V_t	0.043***	(0.006)	0.038***	(0.003)
Δw_t^n	−1.271	(0.742)	−0.808**	(0.353)
Δw_t^p	−1.331***	(0.383)	−0.577**	(0.265)
Δs_t^n	8.318	(4.777)	−3.889	(4.843)
Δs_t^p	−6.672	(5.434)	8.814*	(4.036)
Δt	−0.094	(0.050)	0.093**	(0.034)
#Obs	3092		6953	
R^2_{adj}	0.155		0.159	

	H7Q2			
	Regime 1		Regime 2	
	$DQ^{***} \leq 1.042$		$DQ^{***} > 1.042$	
Variable	Estimate	Std error	Estimate	Std error
Const	0.332	(1.557)	0.668	(2.484)
DQ	−0.748	(1.743)	−1.099	(2.180)
ΔP_{t-1}	−0.307***	(0.026)	−0.303***	(0.023)
ΔP_{t-2}	−0.180***	(0.025)	−0.128***	(0.018)
ΔP_{t-3}	−0.100***	(0.021)	−0.083***	(0.016)
V_t	0.059***	(0.012)	0.021**	(0.008)
Δw_t^n	−0.376	(0.600)	−0.686**	(0.264)
Δw_t^p	−1.471***	(0.430)	−0.622*	(0.322)
Δs_t^n	2.863	(2.657)	−8.559*	(4.051)
Δs_t^p	−2.338	(4.187)	1.674	(2.340)
Δt	−0.145**	(0.046)	0.113***	(0.033)
#Obs	2813		6180	
R^2_{adj}	0.159		0.110	

	H7Q3			
	Regime 1		Regime 2	
	$DQ^{***} \leq 1.053$		$DQ^{***} > 1.053$	
Variable	Estimate	Std error	Estimate	Std error
Const	−1.927	(1.514)	−2.104	(2.772)
DQ	2.532	(1.646)	1.670	(2.429)
ΔP_{t-1}	−0.322***	(0.026)	−0.321***	(0.029)
ΔP_{t-2}	−0.139***	(0.024)	−0.148***	(0.022)
ΔP_{t-3}	−0.061**	(0.022)	−0.093***	(0.021)
V_t	−0.026**	(0.010)	−0.020***	(0.006)
Δw_t^n	−0.111	(0.568)	−0.781*	(0.356)
Δw_t^p	−0.636	(0.335)	−0.281	(0.402)
Δs_t^n	2.767	(2.280)	−10.365*	(4.773)
Δs_t^p	−3.519	(3.005)	−1.861	(1.975)
Δt	−0.085	(0.043)	0.131***	(0.035)
#Obs	3154		6399	
R^2_{adj}	0.111		0.139	

	H7Q4			
	Regime 1		Regime 2	
	$DQ^{***} \leq 1.156$		$DQ^{***} > 1.156$	
Variable	Estimate	Std error	Estimate	Std error
Const	−2.178	(0.781)	−1.899	(5.697)
DQ	2.115	(0.743)	1.423	(4.773)
ΔP_{t-1}	−0.332***	(0.019)	−0.228***	(0.034)
ΔP_{t-2}	−0.154***	(0.016)	−0.101***	(0.029)
ΔP_{t-3}	−0.061	(0.015)	−0.039	(0.033)
V_t	−0.014*	(0.003)	−0.014**	(0.005)
Δw_t^n	−0.888	(0.400)	−0.187	(0.647)
Δw_t^p	−1.075**	(0.307)	0.715	(0.472)
Δs_t^n	1.202	(2.256)	−8.426**	(3.314)
Δs_t^p	−6.350**	(2.088)	−3.801	(2.609)
Δt	0.064	(0.033)	0.164**	(0.053)
#Obs	8308		3173	
R^2_{adj}	0.126		0.120	

$^{*}p < 0.1$; $^{**}p < 0.05$; $^{***}p < 0.01$

Table 2: Estimation results of the benchmark econometric model (1) for intraday price changes ΔP_t of 15-minute contracts H7Q1–4.

	H18Q1			
	Regime 1		Regime 2	
	$DQ \leq 1.135$		$DQ > 1.135$	
Variable	Estimate	Std error	Estimate	Std error
Const	0.151	(0.984)	9.257	(7.735)
DQ	0.075	(0.916)	−7.531	(6.525)
ΔP_{t-1}	-0.278^{**}	(0.039)	-0.431^{**}	(0.174)
ΔP_{t-2}	−0.115	(0.022)	−0.176	(0.166)
ΔP_{t-3}	−0.018	(0.020)	0.077	(0.128)
V_t	−0.003	(0.003)	−0.012	(0.005)
Δw_t^n	−1.831	(0.243)	−0.609	(0.729)
Δw_t^p	−0.539	(0.606)	−2.141	(0.546)
Δs_t^n	−1.823	(1.332)	−2.994	(3.769)
Δs_t^p	−4.223	(1.224)	−2.563	(2.356)
Δt	−0.052	(0.015)	−0.036	(0.042)
#Obs	9790		2403	
R^2_{adj}	0.105		0.191	

	H18Q2			
	Regime 1		Regime 2	
	$DQ^* \leq 1.118$		$DQ^* > 1.118$	
Variable	Estimate	Std error	Estimate	Std error
Const	−0.145	(1.045)	−1.549	(5.186)
DQ	0.180	(0.986)	1.364	(4.503)
ΔP_{t-1}	-0.322^{***}	(0.019)	-0.277^{***}	(0.029)
ΔP_{t-2}	-0.112^{**}	(0.016)	-0.138^{***}	(0.023)
ΔP_{t-3}	−0.063	(0.014)	−0.010	(0.020)
V_t	0.010	(0.006)	−0.006	(0.007)
Δw_t^n	0.101	(0.618)	−3.040	(1.238)
Δw_t^p	-1.736^{**}	(0.371)	0.652	(0.668)
Δs_t^n	−0.848	(1.465)	1.752	(3.483)
Δs_t^p	−1.716	(1.551)	0.654	(1.895)
Δt	−0.016	(0.016)	−0.015	(0.029)
#Obs	7672		2973	
R^2_{adj}	0.121		0.103	

	H18Q3			
	Regime 1		Regime 2	
	$DQ \leq 1.144$		$DQ > 1.144$	
Variable	Estimate	Std error	Estimate	Std error
Const	−0.443	(0.893)	5.784	(9.044)
DQ	0.236	(0.838)	−4.823	(7.749)
ΔP_{t-1}	-0.308^{***}	(0.016)	-0.291^{***}	(0.044)
ΔP_{t-2}	-0.150^{***}	(0.016)	−0.045	(0.032)
ΔP_{t-3}	-0.044^{***}	(0.012)	−0.009	(0.026)
V_t	0.006	(0.007)	−0.008	(0.011)
Δw_t^n	−0.423	(0.326)	-3.505^{***}	(0.822)
Δw_t^p	-1.480^{**}	(0.673)	2.335	(2.162)
Δs_t^n	-4.480^{**}	(1.830)	0.073	(2.401)
Δs_t^p	−0.267	(1.432)	16.354^{**}	(7.125)
Δt	0.018	(0.014)	−0.066	(0.055)
#Obs	9745		1249	
R^2_{adj}	0.112		0.149	

	H18Q4			
	Regime 1		Regime 2	
	$DQ \leq 1.171$		$DQ > 1.171$	
Variable	Estimate	Std error	Estimate	Std error
Const	−0.378	(0.730)	21.412	(39.252)
DQ	0.279	(0.693)	−17.492	(32.591)
ΔP_{t-1}	-0.312^{***}	(0.021)	-0.386^{*}	(0.212)
ΔP_{t-2}	-0.126^{***}	(0.016)	−0.118	(0.148)
ΔP_{t-3}	−0.030	(0.013)	−0.266	(0.101)
V_t	0.001	(0.002)	0.051	(0.027)
Δw_t^n	−1.897	(0.977)	2.568	(5.729)
Δw_t^p	−0.180	(0.297)	−5.008	(3.700)
Δs_t^n	1.935	(1.927)	7.501	(6.666)
Δs_t^p	-4.024^{*}	(1.563)	4.548	(6.819)
Δt	0.008	(0.016)	−0.130	(0.127)
#Obs	12 779		326	
R^2_{adj}	0.114		0.208	

$^{*}p < 0.1$; $^{**}p < 0.05$; $^{***}p < 0.01$

Table 3: Estimation results of the benchmark econometric model (1) for intraday price changes ΔP_t of 15-minute contracts H18Q1–4.

positive relationship between intraday auction prices and expected demands: $P_d^{\mathrm{Auc},(i)}$ increases as $\ell_d^{(i)}$ increases. For high levels of demand, more expensive generation technologies are in use which puts upward pressure on prices. In particular, we may identify two clusters: One cluster encompasses expected demands $\ell < 58$ GW, and the other cluster comprises $\ell \geq 58$ GW. These clusters reflect low and high electricity demand on weekends and weekdays, respectively. Overall, the data points exhibit a fairly wide range of variation which stems from the strongly varying expectation of renewable power infeed.

For the empirical merit order curve $f(\ell)$, we use the exponential function $f(\ell) = \mathrm{e}^{a\,\ell+b}$ following He et al. (2013). Of course other choices for $f(\ell)$ are possible, but we want to keep our model as simple as possible. We fit the exponential function $f(\ell)$ to the empirical intraday auction price $P^{\mathrm{Auc},(i)}$ as a function of expected demand $\ell^{(i)}$. Technically, we minimize the sum of squared errors between the logarithm of the function $f^{\Phi}(\ell)$ implied by the choice of a parameter set $\Phi = \{a, b\}$, and the logarithm of the empirical intraday auction price $P_d^{\mathrm{Auc},(i)}\left(\ell_d^{(i)}\right)$,

$$\min_{\Phi} \sum_{d=1}^{T} \left| \log\left(P_d^{\mathrm{Auc},(i)}\left(\ell_d^{(i)}\right)\right) - \log\left(f^{\Phi}(\ell)\right)\right|^2 . \tag{11}$$

The least squares fit for contract $i =$ H13Q4 is shown in Figure 6. The parameter estimates of a, b for contracts H7, H13, H18, Q1–Q4 each, are reported in Table 4.

We observe an hourly seasonality of the parameter estimates $\hat{a}, \hat{b}$. For contracts H4Q1–H14Q4, the estimates $\hat{a}, \hat{b}$ increase and decrease from the first to the last 15-minute contract within an hour, respectively, whereas for contracts H15Q1–H2Q4, the estimates $\hat{a}, \hat{b}$ decrease and increase, respectively. Thus, the curvature of the empirical merit order curve $f(\ell)$ grows from Q1 to Q4 in each hour during morning and noon hours, whereas it declines from Q1 to Q4 during afternoon and evening hours. This hourly seasonality may be associated with rising and falling demand in the first and second half of the day, respectively, following human activity (Paraschiv, 2013). Consequently, in the first half of the day, more expensive power plants are needed to cover demand in the last than in the first quarter-hour in each hour, whereas in the second half of the day, more expensive power plants are operated in the first than in the last quarter-hour per hour.

Eventually, we take the derivative of the fitted merit-order-curve function $f'^{\,\Phi}(\ell) = \frac{\mathrm{d}f^{\Phi}(\ell)}{\mathrm{d}\ell}$ and substitute empirical expected demands $\ell_d^{(i)}$ into $f'^{\,\Phi}(\ell)$ to obtain empirical merit-order-curve slopes $\xi_d^{(i)} = f'^{\,\Phi}\left(\ell_d^{(i)}\right)$ on days $d = 1, \ldots, T$, for 15-minute contract i.

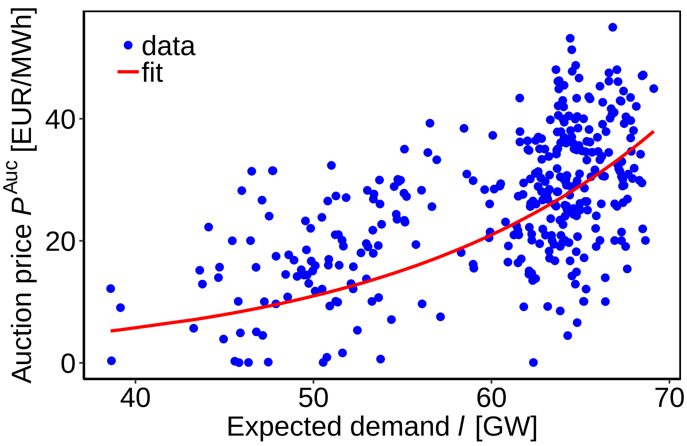

Figure 6: Empirical merit-order-curve function $f(\ell) = \mathrm{e}^{a\,\ell+b}$ (red) fitted to the empirical intraday auction price $P_d^{\mathrm{Auc},(i)}$ as a function of expected demand $\ell_d^{(i)}$ (blue) observed on days $d = 1, \ldots, T$, for 15-minute contract $i =$ H13Q4.

	Parameter			
	a		b	
Contract	Estimate	Std error	Estimate	Std error
H7Q1	0.029	(0.004)	1.632	(0.268)
H7Q2	0.036	(0.002)	1.412	(0.134)
H7Q3	0.045	(0.002)	0.961	(0.125)
H7Q4	0.045	(0.002)	0.940	(0.130)
H13Q1	0.022	(0.002)	2.194	(0.141)
H13Q2	0.037	(0.003)	1.214	(0.201)
H13Q3	0.045	(0.004)	0.548	(0.217)
H13Q4	0.065	(0.006)	-0.856	(0.389)
H18Q1	0.061	(0.005)	-0.372	(0.313)
H18Q2	0.039	(0.003)	1.246	(0.160)
H18Q3	0.021	(0.002)	2.546	(0.109)
H18Q4	0.013	(0.002)	3.074	(0.140)

Table 4: Parameter estimates of a, b of the empirical merit-order-curve function $f(\ell) = \mathrm{e}^{a\,\ell+b}$ for 15-minute contracts H7, H13, H18, Q1–Q4 each.

4.2.2 Model calibration

The estimation results of all 15-minute contracts in hours H13, H7, H18 are presented in Tables 5, 6, 7, respectively. The threshold test shows strong evidence for a threshold effect in the slope of the merit order curve ξ for all contracts in hours H13 and H7, while in hour H18, it indicates a statistically significant threshold effect for contract Q2 and Q3. A merit-order-curve slope of $\xi = 1\ \frac{\text{EUR/MWh}}{\text{GW}}$ implies that a change of 1 GW in expected demand causes a change of 1 EUR/MWh in the intraday auction price. Regime 1 corresponds to a market in which the merit order curve is flat, whereas Regime 2 reflects a market in which the merit order curve is steep. For all contracts, the total sample is split into subsamples of appropriate size and enables us to interpret the estimation results adequately.

The adjusted R^2 ranges between 11% and 22%. Thus, overall, our extended econometric model exhibits higher explanatory power in explaining intraday price changes ΔP_t than the benchmark model by Kiesel and Paraschiv (2017). In particular, our extended model outnumbers the benchmark model's adjusted R^2 for each contract and regime in hours H13 and H7. In hour H18, the extended model only improves the explanation of intraday price changes ΔP_t in either regime compared to the benchmark model.

The estimated coefficients of lagged price changes $\Delta P_{t-1}, \Delta P_{t-2}, \Delta P_{t-3}$ are highly statistically significant and negative in both regimes for all contracts in hours H13 and H7. In hour H18, the higher-order autoregressive terms show less statistical significance. The negative coefficients of lagged price changes suggest mean reversion in the price formation process of 15-minute contracts. We recall that Kiesel and Paraschiv (2017) find less explanatory power of autoregressive terms during noon hours when renewable forecast changes primarily dominate 15-minute intraday trading. We, however, provide evidence of a significant mean reversion effect for noon contracts in 2015.

Overall, in hour H13, the estimated coefficients of price changes of neighboring contracts $\Delta P_t^{(i-2)}, \dots, \Delta P_t^{(i+2)}$ are highly statistically significant and positive in both regimes for all contracts. In hour H7, the estimated coefficients of $\Delta P_t^{(i-2)}, \dots, \Delta P_t^{(i+2)}$ are highly statistically significant and positive in the steep merit-order regime for all contracts as well as in the flat regime for contracts Q3 and Q4. Thus, price changes of neighboring contracts have strong explanatory power and a positive effect on one another. Moreover, we observe that price changes of the nearest neighbors $i \pm 1$ have a stronger impact on price changes of contract i than price changes of next-nearest neighbors $i \pm 2$ [6]. In particular, for the first 15-minute contract Q1 in an hour, price changes $\Delta P_t^{(i+1)}$ of the following contract Q2 have the greatest influence, whereas for the last contract Q4 in that hour, price changes $\Delta P_t^{(i-1)}$ of the preceding contract Q3 exhibit the largest impact. Hence, 15-minute contracts within the same hour are the most important price drivers. In hour H18, the coefficients of $\Delta P_t^{(i-2)}, \ldots, \Delta P_t^{(i+2)}$ are rarely statistically significant.

The coefficients of the intraday auction price P^{Auc} are not significant for all contracts and regimes. This is not surprising since P^{Auc} can merely be considered as an estimate of the initial price of a 15-minute contract in the continuous trading. Thus, it is not expected that P^{Auc} affects continuous trading beyond the first price.

In hour H13, the coefficients of trading volume V_t are significant in the flat merit-order regime for all contracts and in the steep regime for contracts Q1 and Q4. Independent of the regime, they are negative for Q1 and Q2 and positive for Q3 and Q4. This sign profile illustrates the joint hourly seasonality of intraday prices and volumes presented in Section 2.2: As more solar power is generated than the hourly average in Q1 and Q2, there is sell pressure at the beginning of the hour and intraday prices decrease. Conversely, buy pressure increases intraday prices at the end of the hour (Q3 and Q4) when below-average solar power is produced. In hour H7, the coefficients of V_t are significant for all contracts and regimes and we observe the opposite sign pattern: For contracts Q1 and Q2, the coefficients are positive, whereas for Q3 and Q4, they turn negative independent of the regime. Thereby, the positive and negative coefficients reflect buy and sell pressure at the beginning and end of the hour, respectively. In hour H18, the coefficients of V_t are not significant. In general, we do not find an asymmetric adjustment of intraday price changes ΔP_t to trading volumes V_t.

Overall, the coefficients of negative wind forecast changes Δw_t^n are significant and negative in the steep merit-order regime for all contracts. The negative sign is economically meaningful as electricity prices should increase if less wind power is forecasted. In hour H13, the coefficients of positive wind forecast changes Δw_t^p are only significant and negative in the steep regime for Q1 and Q3. In hour H7, the coefficients of Δw_t^p are significant and negative in the flat regime for all contracts as well as in the steep regime for Q1 and Q2, while in hour H18, they are significant and negative in both regimes for Q3. The negative coefficients imply that electricity prices decline in the wake of rising wind power infeed, which is consistent with our intuition. No asymmetry in the coefficients of wind forecast changes between the regimes is observed. We conclude that generally wind forecast errors have explanatory power to explaining intraday price changes ΔP_t.

The coefficients of negative solar forecast changes Δs_t^n are significant and negative in the steep merit-order regime, but not significant in the flat regime for contracts in hours H13 and H7. In hour H18, the coefficients of Δs_t^n are significant in both regimes for Q3. In the steep regimes, the coefficients of Δs_t^n are at least two times larger by absolute value than in the flat regimes. This reflects the fact that renewable forecast changes affect electricity prices more severely in the steep than in the flat merit-order regime. In hour H13, the coefficients of positive solar forecast changes Δs_t^p are significant and negative in both regimes for contracts Q1 and Q2. In hour H7, the coefficients of Δs_t^p are significant and negative in both regimes for Q4, while in hour H18, they are generally not significant. The negative coefficients of both negative and positive forecast errors of solar power production are reasonable: A lower expectation of solar power infeed should increase electricity prices, whereas a larger solar power prediction decreases electricity prices.

Generally, renewable forecast changes are more significant in the steep than in the flat merit-order regime. When the market is in the steep merit-order regime, market participants rely

[6] The terms nearest and next-nearest neighbors are motivated from physics where a nearest- and next-nearest-neighbor interaction exists.

on the use of more expensive power generation technologies, which sets additional pressure on them to balance the volatile renewable energies on the intraday market.

Eventually, intraday trading of 15-minute contracts is driven by both price-related and fundamental variables at noon, while the price-related variables have a slight surplus importance. For morning and evening contracts, however, intraday price changes are predominantly influenced by past, idiosyncratic price information and the price information of neighboring contracts.

5 Conclusion

This paper develops an econometric price model with fundamental impacts for intraday electricity markets of 15-minute contracts. We analyze a novel and unique data set of high-frequency transaction data, fundamental supply and demand data, and intradaily updated forecasts of wind and solar power generation. The nature of our data set allows the model specification to solely include *ex-ante* market information.

We perform an empirical exploration of transaction prices and trading volumes of 15-minute contracts. Empirical evidence suggests that, on average, transaction prices of 15-minute contracts exhibit a sawtooth-shaped and trading volumes a U-shaped hourly seasonality. Moreover, liquidity increases sharply within the last trading hour before gate closure. Our empirical analysis also indicates that renewable forecast updates are reflected in intraday prices within one trading minute.

We refine the econometric model by Kiesel and Paraschiv (2017) along three dimensions by incorporating: (i) the slope of the merit order curve, (ii) price changes of neighboring 15-minute contracts, (iii) the 15-minute intraday auction price. We calibrate our econometric model to market data for a selection of morning, noon, and evening contracts. A threshold regression model is used to examine how 15-minute intraday trading depends on the slope of the merit order curve.

Our estimation results reveal that autoregressive price changes up to the third order are highly statistically significant and negative, independent of the time of day. This behavior provides clear evidence of mean reversion in the price formation mechanism of 15-minute contracts. Additionally, price changes of neighboring contracts exhibit strong explanatory power and a positive impact on price changes of a given 15-minute contract. We observe an asymmetric effect of positive and negative renewable forecast changes on intraday prices depending on the merit-order-curve slope: Renewable forecasts affect electricity prices more severely in the steep than in the flat merit-order regime. In general, renewable forecast changes have a higher explanatory power for pricing noon than morning and evening contracts, but price information is the key driver of 15-minute intraday trading. Overall, we conclude that the importance of influencing factors on the intraday electricity market has changed from fundamental towards trade-related factors.

As our econometric model exclusively involves *ex-ante* market knowledge, it allows to develop trading strategies for intraday electricity markets, tailor-made for each contract. Furthermore, it helps to design forecasting models for single intraday transaction prices in the continuous trading – to our knowledge, an unexplored territory of scientific research hitherto. Moreover, our article provides a valuable step towards the optimization of the bidding behavior on intraday markets. Eventually, our insights should prove useful to energy companies within the process of automating intraday electricity trading.

	H13Q1			
	Regime 1		Regime 2	
	$\xi^{**} \leq 0.689$		$\xi^{**} > 0.689$	
Variable	Estimate	Std error	Estimate	Std error
Const	-1.504	(1.643)	-0.867	(0.911)
ξ	2.610	(2.672)	1.021	(1.054)
ΔP_{t-1}	-0.363^{***}	(0.040)	-0.311^{***}	(0.018)
ΔP_{t-2}	-0.188^{***}	(0.030)	-0.131^{***}	(0.015)
ΔP_{t-3}	-0.120^{***}	(0.035)	-0.088^{***}	(0.015)
$\Delta P_t^{(i-2)}$	0.064^{**}	(0.025)	0.020	(0.010)
$\Delta P_t^{(i-1)}$	0.063^{**}	(0.025)	0.051^{***}	(0.012)
$\Delta P_t^{(i+1)}$	0.144^{***}	(0.034)	0.136^{***}	(0.016)
$\Delta P_t^{(i+2)}$	0.049^{**}	(0.024)	0.036^{***}	(0.011)
P^{Auc}	0.000	(0.015)	0.002	(0.006)
V_t	-0.025^{***}	(0.006)	-0.017^{***}	(0.003)
Δw_t^n	-0.528	(0.378)	-1.135^{***}	(0.208)
Δw_t^p	-0.554	(0.421)	-0.688^{**}	(0.247)
Δs_t^n	0.852	(0.362)	-1.604^{***}	(0.417)
Δs_t^p	-2.842^{***}	(0.513)	-1.860^{***}	(0.403)
Δt	0.098^{***}	(0.029)	0.058^{***}	(0.016)
#Obs	3131		9922	
R^2_{adj}	0.201		0.190	

	H13Q2			
	Regime 1		Regime 2	
	$\xi^{***} \leq 0.912$		$\xi^{***} > 0.912$	
Variable	Estimate	Std error	Estimate	Std error
Const	-0.201	(1.225)	0.304	(0.734)
ξ	0.931	(1.622)	-0.371	(0.548)
ΔP_{t-1}	-0.332^{***}	(0.034)	-0.322^{***}	(0.023)
ΔP_{t-2}	-0.172^{***}	(0.028)	-0.132^{***}	(0.016)
ΔP_{t-3}	-0.058^{*}	(0.032)	-0.021	(0.020)
$\Delta P_t^{(i-2)}$	0.093^{***}	(0.027)	0.053^{***}	(0.014)
$\Delta P_t^{(i-1)}$	0.212^{***}	(0.034)	0.168^{***}	(0.021)
$\Delta P_t^{(i+1)}$	0.109^{***}	(0.025)	0.140^{***}	(0.024)
$\Delta P_t^{(i+2)}$	0.021	(0.030)	0.042	(0.016)
P^{Auc}	-0.011	(0.021)	0.006	(0.007)
V_t	-0.022^{*}	(0.010)	-0.007	(0.007)
Δw_t^n	-0.564	(0.280)	-1.179^{***}	(0.202)
Δw_t^p	-0.390	(0.346)	-0.228	(0.188)
Δs_t^n	0.181	(0.344)	-1.750^{***}	(0.374)
Δs_t^p	-2.629^{***}	(0.398)	-1.485^{***}	(0.376)
Δt	0.029	(0.029)	0.027	(0.016)
#Obs	2759		9284	
R^2_{adj}	0.188		0.198	

	H13Q3			
	Regime 1		Regime 2	
	$\xi^{**} \leq 1.324$		$\xi^{**} > 1.324$	
Variable	Estimate	Std error	Estimate	Std error
Const	-0.687	(0.390)	-1.215	(0.986)
ξ	1.016	(0.497)	0.707	(0.649)
ΔP_{t-1}	-0.287^{***}	(0.024)	-0.306^{***}	(0.023)
ΔP_{t-2}	-0.143^{***}	(0.024)	-0.165^{***}	(0.021)
ΔP_{t-3}	-0.058^{*}	(0.018)	-0.080^{***}	(0.017)
$\Delta P_t^{(i-2)}$	0.061^{***}	(0.017)	0.044	(0.017)
$\Delta P_t^{(i-1)}$	0.059^{***}	(0.016)	0.147^{***}	(0.031)
$\Delta P_t^{(i+1)}$	0.147^{***}	(0.021)	0.230^{***}	(0.029)
$\Delta P_t^{(i+2)}$	0.075^{**}	(0.019)	0.044	(0.014)
P^{Auc}	-0.016	(0.017)	-0.004	(0.008)
V_t	0.012^{*}	(0.006)	0.014	(0.004)
Δw_t^n	-1.029	(0.333)	-0.753^{***}	(0.205)
Δw_t^p	-0.094	(0.184)	-0.594^{**}	(0.261)
Δs_t^n	0.133	(0.355)	-2.276^{***}	(0.437)
Δs_t^p	-1.967^{***}	(0.319)	-0.943	(0.474)
Δt	-0.011	(0.021)	0.027	(0.021)
#Obs	5626		7190	
R^2_{adj}	0.129		0.214	

	H13Q4			
	Regime 1		Regime 2	
	$\xi^{**} \leq 0.995$		$\xi^{**} > 0.995$	
Variable	Estimate	Std error	Estimate	Std error
Const	-0.396	(0.541)	-0.183	(0.377)
ξ	-0.111	(0.800)	-0.196	(0.204)
ΔP_{t-1}	-0.331^{***}	(0.027)	-0.298^{***}	(0.019)
ΔP_{t-2}	-0.176^{***}	(0.025)	-0.135^{***}	(0.014)
ΔP_{t-3}	-0.095^{***}	(0.023)	-0.071^{***}	(0.013)
$\Delta P_t^{(i-2)}$	0.038	(0.018)	0.043^{***}	(0.013)
$\Delta P_t^{(i-1)}$	0.114^{***}	(0.021)	0.168^{***}	(0.022)
$\Delta P_t^{(i+1)}$	0.069^{***}	(0.021)	0.062^{***}	(0.013)
$\Delta P_t^{(i+2)}$	0.045^{**}	(0.018)	0.061^{***}	(0.014)
P^{Auc}	0.011	(0.014)	0.010^{*}	(0.006)
V_t	0.012^{*}	(0.005)	0.013^{***}	(0.003)
Δw_t^n	-1.473^{***}	(0.396)	-1.188^{***}	(0.231)
Δw_t^p	-0.366	(0.329)	-0.407	(0.222)
Δs_t^n	-0.211	(0.377)	-2.403^{***}	(0.406)
Δs_t^p	-1.232	(0.481)	-0.259	(0.496)
Δt	-0.068^{*}	(0.028)	-0.031	(0.019)
#Obs	3893		11 261	
R^2_{adj}	0.144		0.182	

$^{*}p < 0.1$; $^{**}p < 0.05$; $^{***}p < 0.01$

Table 5: Estimation results of the extended econometric model (2) for intraday price changes ΔP_t of 15-minute contracts H13Q1–4.

	H7Q1			
	Regime 1		Regime 2	
	$\xi^{***} \leq 0.722$		$\xi^{***} > 0.722$	
Variable	Estimate	Std error	Estimate	Std error
Const	2.057	(1.198)	−0.224	(1.234)
ξ	-5.064^{**}	(1.958)	−0.541	(1.179)
ΔP_{t-1}	-0.354^{***}	(0.032)	-0.390^{***}	(0.023)
ΔP_{t-2}	-0.179^{***}	(0.032)	-0.184^{***}	(0.020)
ΔP_{t-3}	-0.114^{***}	(0.029)	-0.064^{***}	(0.018)
$\Delta P_t^{(i-2)}$	0.024	(0.022)	0.032^{**}	(0.012)
$\Delta P_t^{(i-1)}$	−0.001	(0.026)	0.012	(0.014)
$\Delta P_t^{(i+1)}$	0.155^{***}	(0.025)	0.101^{***}	(0.015)
$\Delta P_t^{(i+2)}$	−0.011	(0.022)	0.060^{***}	(0.016)
P^{Auc}	0.016	(0.016)	−0.009	(0.010)
V_t	0.040^{***}	(0.006)	0.037^{***}	(0.003)
Δw_t^n	0.202	(0.828)	-1.234^{***}	(0.277)
Δw_t^p	-1.388^{***}	(0.386)	-0.661^{***}	(0.242)
Δs_t^n	6.741	(4.483)	−5.254	(3.889)
Δs_t^p	0.415	(5.261)	6.708^{*}	(4.008)
Δt	-0.089^{*}	(0.049)	0.085^{**}	(0.032)
#Obs	2923		7122	
R^2_{adj}	0.186		0.188	

	H7Q2			
	Regime 1		Regime 2	
	$\xi^{***} \leq 1.050$		$\xi^{***} > 1.050$	
Variable	Estimate	Std error	Estimate	Std error
Const	0.233	(0.995)	−0.429	(0.954)
ξ	−0.567	(1.232)	−0.084	(0.605)
ΔP_{t-1}	-0.341^{***}	(0.028)	-0.322^{***}	(0.021)
ΔP_{t-2}	-0.193^{***}	(0.026)	-0.149^{***}	(0.017)
ΔP_{t-3}	-0.116^{***}	(0.022)	-0.094^{***}	(0.015)
$\Delta P_t^{(i-2)}$	0.024	(0.021)	0.014	(0.014)
$\Delta P_t^{(i-1)}$	0.201^{***}	(0.029)	0.104^{***}	(0.017)
$\Delta P_t^{(i+1)}$	0.065^{***}	(0.024)	0.137^{***}	(0.019)
$\Delta P_t^{(i+2)}$	0.050	(0.030)	0.047^{***}	(0.017)
P^{Auc}	0.002	(0.018)	−0.002	(0.013)
V_t	0.054^{***}	(0.012)	0.023^{***}	(0.008)
Δw_t^n	0.384	(0.448)	-0.855^{***}	(0.217)
Δw_t^p	-1.367^{***}	(0.437)	-0.658^{**}	(0.285)
Δs_t^n	0.411	(2.432)	-9.320^{***}	(3.522)
Δs_t^p	0.384	(3.563)	1.298	(2.208)
Δt	-0.154^{***}	(0.044)	0.101^{***}	(0.030)
#Obs	2573		6420	
R^2_{adj}	0.218		0.157	

	H7Q3			
	Regime 1		Regime 2	
	$\xi^{***} \leq 1.403$		$\xi^{***} > 1.403$	
Variable	Estimate	Std error	Estimate	Std error
Const	−0.498	(0.770)	0.217	(0.750)
ξ	0.995	(0.881)	−0.219	(0.376)
ΔP_{t-1}	-0.364^{***}	(0.025)	-0.342^{***}	(0.027)
ΔP_{t-2}	-0.169^{***}	(0.025)	-0.172^{***}	(0.020)
ΔP_{t-3}	-0.061^{**}	(0.022)	-0.108^{***}	(0.019)
$\Delta P_t^{(i-2)}$	0.068^{**}	(0.024)	0.052^{***}	(0.015)
$\Delta P_t^{(i-1)}$	0.063^{**}	(0.020)	0.102^{***}	(0.015)
$\Delta P_t^{(i+1)}$	0.187^{***}	(0.027)	0.147^{***}	(0.019)
$\Delta P_t^{(i+2)}$	0.087^{**}	(0.029)	0.070^{***}	(0.026)
P^{Auc}	−0.001	(0.019)	0.000	(0.012)
V_t	-0.029^{**}	(0.010)	-0.018^{***}	(0.006)
Δw_t^n	0.479	(0.429)	-0.769^{**}	(0.342)
Δw_t^p	-0.686^{*}	(0.350)	−0.190	(0.347)
Δs_t^n	0.724	(1.919)	-10.354^{**}	(4.116)
Δs_t^p	−1.730	(2.524)	−3.032	(1.680)
Δt	-0.112^{**}	(0.040)	0.127^{***}	(0.030)
#Obs	2694		6859	
R^2_{adj}	0.189		0.189	

	H7Q4			
	Regime 1		Regime 2	
	$\xi^{***} \leq 1.459$		$\xi^{***} > 1.459$	
Variable	Estimate	Std error	Estimate	Std error
Const	−0.855	(0.684)	0.421	(0.645)
ξ	1.118	(0.736)	−0.456	(0.320)
ΔP_{t-1}	-0.363^{***}	(0.031)	-0.319^{***}	(0.019)
ΔP_{t-2}	-0.193^{***}	(0.028)	-0.148^{***}	(0.017)
ΔP_{t-3}	-0.063^{***}	(0.023)	-0.069^{***}	(0.019)
$\Delta P_t^{(i-2)}$	0.049^{*}	(0.019)	0.077^{***}	(0.012)
$\Delta P_t^{(i-1)}$	0.150^{***}	(0.024)	0.160^{***}	(0.019)
$\Delta P_t^{(i+1)}$	0.036	(0.029)	0.034^{*}	(0.018)
$\Delta P_t^{(i+2)}$	0.052^{*}	(0.028)	0.065^{***}	(0.015)
P^{Auc}	0.002	(0.015)	0.006	(0.009)
V_t	-0.017^{**}	(0.005)	-0.013^{***}	(0.003)
Δw_t^n	1.038	(0.649)	-0.894^{**}	(0.352)
Δw_t^p	-1.058^{**}	(0.364)	−0.285	(0.363)
Δs_t^n	0.848	(2.429)	-8.062^{***}	(2.585)
Δs_t^p	-5.688^{**}	(2.541)	-3.543^{*}	(1.621)
Δt	−0.050	(0.044)	0.144^{***}	(0.029)
#Obs	3407		8074	
R^2_{adj}	0.190		0.177	

$^{*}p < 0.1$; $^{**}p < 0.05$; $^{***}p < 0.01$

Table 6: Estimation results of the extended econometric model (2) for intraday price changes ΔP_t of 15-minute contracts H7Q1–4.

	H18Q1			
	Regime 1		Regime 2	
	$\xi \leq 2.546$		$\xi > 2.546$	
Variable	Estimate	Std error	Estimate	Std error
Const	0.162	(0.252)	4.401	(3.252)
ξ	0.051	(0.140)	−1.542	(1.226)
ΔP_{t-1}	-0.287^{***}	(0.036)	-0.434^{**}	(0.191)
ΔP_{t-2}	-0.117^{***}	(0.021)	−0.197	(0.181)
ΔP_{t-3}	−0.013	(0.019)	0.052	(0.137)
$\Delta P_t^{(i-2)}$	−0.004	(0.009)	0.017	(0.030)
$\Delta P_t^{(i-1)}$	−0.002	(0.007)	−0.004	(0.017)
$\Delta P_t^{(i+1)}$	0.030^{***}	(0.008)	−0.046	(0.037)
$\Delta P_t^{(i+2)}$	0.004	(0.009)	−0.037	(0.031)
P^{Auc}	0.003	(0.005)	0.004	(0.017)
V_t	-0.005^{*}	(0.003)	−0.001	(0.006)
Δw_t^n	-1.743^{**}	(0.367)	−0.808	(0.949)
Δw_t^p	−0.622	(0.588)	-1.936^{**}	(0.865)
Δs_t^n	−2.191	(1.313)	2.391	(2.441)
Δs_t^p	-4.131^{***}	(1.094)	1.285	(1.796)
Δt	-0.053^{***}	(0.016)	−0.038	(0.038)
#Obs	10 142		2051	
R^2_{adj}	0.113		0.187	

	H18Q2			
	Regime 1		Regime 2	
	$\xi^{**} \leq 1.906$		$\xi^{**} > 1.906$	
Variable	Estimate	Std error	Estimate	Std error
Const	0.031	(0.325)	1.318	(12.363)
ξ	0.133	(0.251)	−0.782	(6.228)
ΔP_{t-1}	-0.323^{***}	(0.016)	-0.163^{***}	(0.049)
ΔP_{t-2}	-0.127^{***}	(0.014)	−0.026	(0.043)
ΔP_{t-3}	−0.055	(0.012)	0.019	(0.042)
$\Delta P_t^{(i-2)}$	0.004	(0.006)	−0.013	(0.021)
$\Delta P_t^{(i-1)}$	0.017^{**}	(0.007)	0.018	(0.036)
$\Delta P_t^{(i+1)}$	0.007	(0.010)	−0.055	(0.029)
$\Delta P_t^{(i+2)}$	0.003	(0.009)	0.011	(0.023)
P^{Auc}	−0.005	(0.007)	0.007	(0.029)
V_t	0.006	(0.005)	−0.004	(0.021)
Δw_t^n	−0.120	(0.489)	−5.117	(0.573)
Δw_t^p	-1.352^{***}	(0.506)	1.639	(1.776)
Δs_t^n	−1.676	(1.299)	7.783	(1.173)
Δs_t^p	−1.059	(1.268)	0.206	(1.767)
Δt	−0.010	(0.014)	−0.101	(0.040)
#Obs	10 072		573	
R^2_{adj}	0.117		0.146	

	H18Q3			
	Regime 1		Regime 2	
	$\xi^{*} \leq 1.037$		$\xi^{*} > 1.037$	
Variable	Estimate	Std error	Estimate	Std error
Const	−1.037	(0.605)	−18.093	(14.430)
ξ	0.725	(0.745)	17.247	(13.490)
ΔP_{t-1}	-0.318^{***}	(0.017)	-0.264^{***}	(0.035)
ΔP_{t-2}	-0.144^{***}	(0.016)	-0.112^{**}	(0.029)
ΔP_{t-3}	-0.043^{***}	(0.012)	−0.031	(0.026)
$\Delta P_t^{(i-2)}$	0.006	(0.007)	−0.021	(0.027)
$\Delta P_t^{(i-1)}$	0.007	(0.008)	0.003	(0.016)
$\Delta P_t^{(i+1)}$	0.005	(0.009)	0.064	(0.021)
$\Delta P_t^{(i+2)}$	0.002	(0.004)	0.030	(0.017)
P^{Auc}	0.005	(0.008)	−0.003	(0.017)
V_t	0.008	(0.006)	−0.021	(0.010)
Δw_t^n	−0.413	(0.389)	-2.264^{***}	(0.759)
Δw_t^p	-1.225^{*}	(0.619)	-3.952^{**}	(1.315)
Δs_t^n	-4.195^{**}	(1.641)	7.669^{***}	(0.978)
Δs_t^p	3.485	(3.236)	-12.870^{***}	(1.538)
Δt	0.010	(0.017)	0.045	(0.032)
#Obs	9597		1397	
R^2_{adj}	0.113		0.126	

	H18Q4			
	Regime 1		Regime 2	
	$\xi \leq 0.632$		$\xi > 0.632$	
Variable	Estimate	Std error	Estimate	Std error
Const	−0.864	(1.401)	−2.063	(2.029)
ξ	1.307	(2.499)	1.617	(3.013)
ΔP_{t-1}	-0.303^{***}	(0.023)	-0.333^{***}	(0.045)
ΔP_{t-2}	-0.152^{***}	(0.020)	−0.107	(0.032)
ΔP_{t-3}	−0.012	(0.017)	−0.081	(0.030)
$\Delta P_t^{(i-2)}$	−0.001	(0.010)	−0.014	(0.011)
$\Delta P_t^{(i-1)}$	0.009	(0.010)	0.044	(0.012)
$\Delta P_t^{(i+1)}$	−0.002	(0.008)	0.009	(0.004)
$\Delta P_t^{(i+2)}$	−0.001	(0.008)	0.010	(0.010)
P^{Auc}	0.004	(0.009)	0.013	(0.007)
V_t	0.000	(0.003)	0.003	(0.003)
Δw_t^n	−1.041	(0.699)	−2.165	(1.214)
Δw_t^p	−0.461	(1.040)	−0.225	(0.349)
Δs_t^n	0.633	(2.239)	0.440	(3.082)
Δs_t^p	−2.177	(1.714)	−5.394	(2.870)
Δt	−0.023	(0.020)	0.035	(0.021)
#Obs	5835		7270	
R^2_{adj}	0.111		0.133	

$^{*}p < 0.1$; $^{**}p < 0.05$; $^{***}p < 0.01$

Table 7: Estimation results of the extended econometric model (2) for intraday price changes ΔP_t of 15-minute contracts H18Q1–4.

Acknowledgements

Florentina Paraschiv thanks the funding from *Adolf Øiens Donasjonsfond* Energizing New Computational Frontiers [grant number L10079] and the Isaac Newton Institute for Mathematical Sciences for its hospitality during the programme "The mathematics of energy systems" which was supported by the Engineering and Physical Sciences Research Council (EPSRC) [grant number EP/R014604/1]. This work has been performed within the +CityxChange (Positive City ExChange, https://cityxchange.eu/) project under the Smart Cities and Communities topic which was supported by the European Union's Horizon 2020 Research and Innovation programme [grant number 824260]. Florentina Paraschiv's research was financially supported by Innosuisse as part of the activities within SCCER CREST.

Appendices

A Data

We provide a summary of explanatory variables, granularities, detailed descriptions, and data sources in Table A.1.

References

Beran, P., Pape, C., and Weber, C. (2019). Modelling German electricity wholesale spot prices with a parsimonious fundamental model – Validation & application. *Utilities Policy*, 58:27–39.

Burger, M., Klar, B., Müller, A., and Schindlmayr, G. (2004). A spot market model for pricing derivatives in electricity markets. *Quantitative Finance*, 4(1):109–122.

EPEX SPOT SE (2015). Press release: EPEX SPOT and ECC successfully reduce lead time on all intraday markets. https://www.epexspot.com/sites/default/files/download_center_files/2015-07-16_EPEX%20SPOT_Lead%20time%20reduction.pdf. (Accessed on Jan 16, 2020).

EPEX SPOT SE (2017). Press release: Exchange Council approves the introduction of 15-minute contracts on the Belgian and Dutch market – Trading until delivery to be launched on the German market on 14 June 2017. https://www.epexspot.com/sites/default/files/download_center_files/170612_EPEX%20SPOT_Exchange%20Council.pdf. (Accessed on Jan 16, 2020).

European Energy Exchange AG (2016a). EEX annual report 2015. https://www.eex.com/blob/16500/ff13c25a4813320ff521bf67ac397e73/eex-gb-2015-en-data.pdf. (Accessed on Mar 1, 2019).

European Energy Exchange AG (2016b). EPEX SPOT DE 15-minute intraday auction market data. https://www.eex.com.

European Energy Exchange AG (2016c). EPEX SPOT DE/AT 15-minute continuous intraday market transaction data. https://www.eex.com.

European Energy Exchange AG Transparency Platform (2016). Available generation capacity data. https://www.eex-transparency.com.

European Network of Transmission System Operators for Electricity Transparency Platform (2016). Day-ahead total load forecast data. https://transparency.entsoe.eu.

Variable [Unit] (*Granularity*)	**Description**	**Source**
Transaction price P_t [EUR/MWh] (*1-minute*)	Transaction price of 15-minute contracts traded on the German continuous intraday power market at EPEX SPOT SE	European Energy Exchange AG (2016c)
Trading volume V_t [MW] (*1-minute*)	Trading volume of 15-minute contracts traded on the German continuous intraday power market at EPEX SPOT SE	European Energy Exchange AG (2016c)
Auction price P^{Auc} [EUR/MWh] (*quarter-hourly*)	Market clearing price of 15-minute contracts traded in the German 15-minute intraday auction at EPEX SPOT SE	European Energy Exchange AG (2016b)
Wind power forecast w_t [GW] (*quarter-hourly*)	Intradaily updated forecast of wind power generation for each quarter-hour on the delivery day in Germany	EWE TRADING GmbH (2016)
Solar power forecast s_t [GW] (*quarter-hourly*)	Intradaily updated forecast of solar power generation for each quarter-hour on the delivery day in Germany	EWE TRADING GmbH (2016)
Expected demand l [GW] (*quarter-hourly*)	Day-ahead total load forecast for each quarter-hour on the delivery day in Germany (published: daily at 10 AM)	European Network of Transmission System Operators for Electricity Transparency Platform (2016)
Expected conventional capacity c [GW] (*daily*)	Expected daily average of available generation capacity of conventional power plants on the delivery day in Germany (published: daily at 10 AM)	European Energy Exchange AG Transparency Platform (2016)

Table A.1: Summary of explanatory variables, granularities, detailed descriptions, and data sources. Variables indexed by t vary over the continuous intraday trading session of a 15-minute contract.

EWE TRADING GmbH (2016). Intradaily updated forecast data of wind and solar power generation. https://www.ewe.com.

Frauendorfer, K., Paraschiv, F., and Schürle, M. (2018). Cross-border effects on Swiss electricity prices in the light of the energy transition. *Energies*, 11(9):2188.

Glas, S., Kiesel, R., Kolkmann, S., Kremer, M., Graf von Luckner, N., Ostmeier, L., Urban, K., and Weber, C. (2020). Intraday renewable electricity trading: Advanced modeling and numerical optimal control. *Journal of Mathematics in Industry*, 10(1):1–17.

Graf von Luckner, N. and Kiesel, R. (2020). Modeling market order arrivals on the intraday market for electricity deliveries in Germany with the Hawkes process. https://ssrn.com/abstract=3526795. (Accessed on Jan 31, 2020).

Hansen, B. E. (2000). Sample splitting and threshold estimation. *Econometrica*, 68(3):575–603.

He, Y., Hildmann, M., Herzog, F., and Andersson, G. (2013). Modeling the merit order curve of the European energy exchange power market in Germany. *IEEE Transactions on Power Systems*, 28(3):3155–3164.

Kallabis, T., Pape, C., and Weber, C. (2016). The plunge in German electricity futures prices – Analysis using a parsimonious fundamental model. *Energy Policy*, 95:280–290.

Karakatsani, N. V. and Bunn, D. W. (2010). Fundamental and behavioural drivers of electricity price volatility. *Studies in Nonlinear Dynamics & Econometrics*, 14(4).

Kath, C. and Ziel, F. (2018). The value of forecasts: Quantifying the economic gains of accurate quarter-hourly electricity price forecasts. *Energy Economics*, 76:411–423.

Kiesel, R. and Paraschiv, F. (2017). Econometric analysis of 15-minute intraday electricity prices. *Energy Economics*, 64:77–90.

Kremer, M. (2020). thrreg: Threshold regression model. https://github.com/mlkremer/thrreg. R package version 0.1.0.

Märkle-Huß, J., Feuerriegel, S., and Neumann, D. (2018). Contract durations in the electricity market: Causal impact of 15 min trading on the EPEX SPOT market. *Energy Economics*, 69:367–378.

Pape, C., Hagemann, S., and Weber, C. (2016). Are fundamentals enough? Explaining price variations in the German day-ahead and intraday power market. *Energy Economics*, 54:376–387.

Paraschiv, F. (2013). Price dynamics in electricity markets. In Kovacevic, R., Pflug, G. C., and Vespucci, M. T., editors, *Handbook of Risk Management in Energy Production and Trading*, volume 199 of *International Series in Operations Research & Management Science*, pages 47–69. Springer Boston MA.

Wagner, T. (2018). emarketcrawlr: Crawling energy market data at EPEX SPOT (intraday trading, intraday auction, day-ahead auction). https://github.com/wagnertimo/emarketcrawlR. R package version 0.1.0.